

The Effect of Charge-Transfer Complexation/ π -Stacking Interactions in Lowering the Activation Barrier of the Bergman Cyclization

Amit Basak,^{*[a]} Subhendu Sekhar Bag,^[a] and Amit K. Das^[b]

Keywords: Cyclization / Charge transfer / Enediynes / Stacking interactions / UV/Vis spectroscopy

To elaborate the concept of weak interactions and their effect on Bergman Cyclization (BC), several 1,2-dikynyl benzenes incorporating various combinations of donor and acceptor units in the two arms of the enediynes were designed and synthesized, and their charge-transfer interactions followed by UV/Vis spectroscopy. The thermal reactivities, as studied by DSC, show an increase in reactivity for the donor/acceptor

or donor/donor combinations relative to the acceptor/acceptor pair. Such an increase in reactivity can be explained on the basis of intramolecular charge transfer and π -stacking interactions between the two arms, which may lower the distance between the two acetylenic ends.

(© Wiley-VCH Verlag GmbH & Co. KGaA, 69451 Weinheim, Germany, 2005)

More than fifty years ago, Mulliken^[1] suggested that charge-transfer (CT) complexes “may afford new possibilities for understanding intermolecular interactions in biological systems”. This statement proved to be true after several biochemical phenomena were explained on the basis of CT complex formation.^[2–5] CT complexes arising from the interaction of aromatic π -donor and -acceptor molecules have been studied extensively. However, fewer intramolecular CT analogs have been reported, primarily of the cyclophane type, in which the donor and acceptor portions are locked together in a rather rigid arrangement.^[6] More flexible intramolecular CT complexes have been reported in a recent communication, whereby a cyclohexane skeleton is substituted at adjacent *trans* positions with aromatic donor and acceptor groups.^[7] Besides charge-transfer interactions, attractive, nonbonding interactions between aromatic units (π -stacking) play a central role in many areas of chemistry and biochemistry, the most notable ones being in molecular recognition and self-assembly,^[8] in base-pair stacking in DNA,^[9] and in controlling the tertiary structure of proteins,^[10] and hence are of interest to all realms of chemistry and biology. The activity profiles of the well-known, medically important enediynes are greatly perturbed by weak interactions.^[11] Jones et al.^[12] have shown that strong electron-withdrawing groups increase the barrier for Bergman cyclization, while σ -donating groups decrease it; π -conjugation, in particular donation, has little effect. In a recent paper Alabugin^[13] evaluated the stereoelectronic effects in cyclohexane-, 1,3-dioxane-, 1,3-oxathiane-, and 1,3-dithiane-

based enediynes. Zaleski et al.^[14] have shown how dramatically the steric influences of the functional groups at the termini of acyclic enediynes can affect the Bergman cyclization (BC) temperatures of the resulting compounds. In this communication, we wish to describe, for the first time, the synthesis and characterization of a series of donor–acceptor (D/A) containing 1,2-dialkynylbenzenes (Figure 1) and the effect of CT complexation and π – π interactions on the kinetics of the BC. The corresponding D/D and A/A counterparts were also synthesized to compare the reactivities towards BC. Incidentally, aromatic 1,2-dialkynyl systems have been considered in the literature^[15] to be a variant of

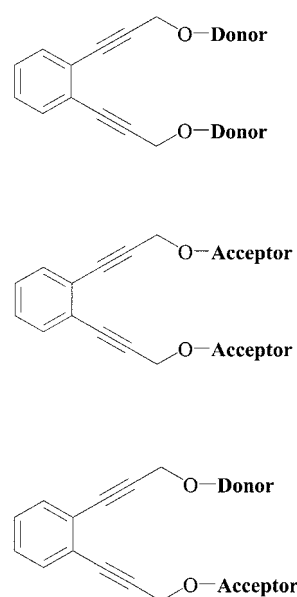


Figure 1. Representation of donor–acceptor-containing enediynyl compounds.

[a] Bioorganic Laboratory, Department of Chemistry, Kharagpur-721302, India

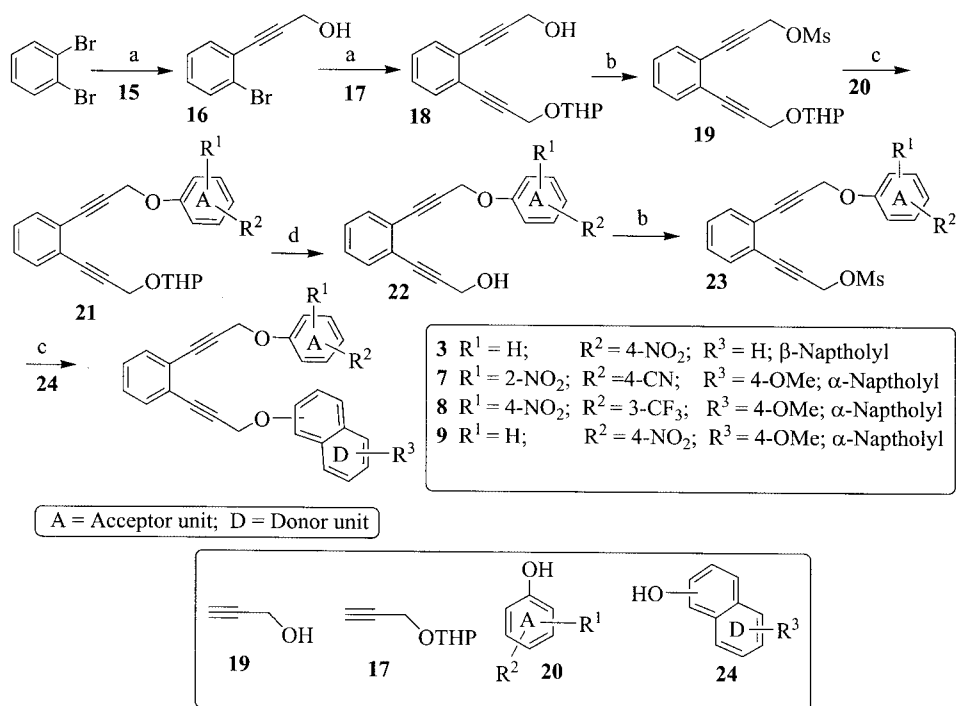
[b] Department of Biotechnology, Indian Institute of Technology, Kharagpur-721302, India

Supporting information for this article is available on the WWW under <http://www.eurjoc.org> or from the author.

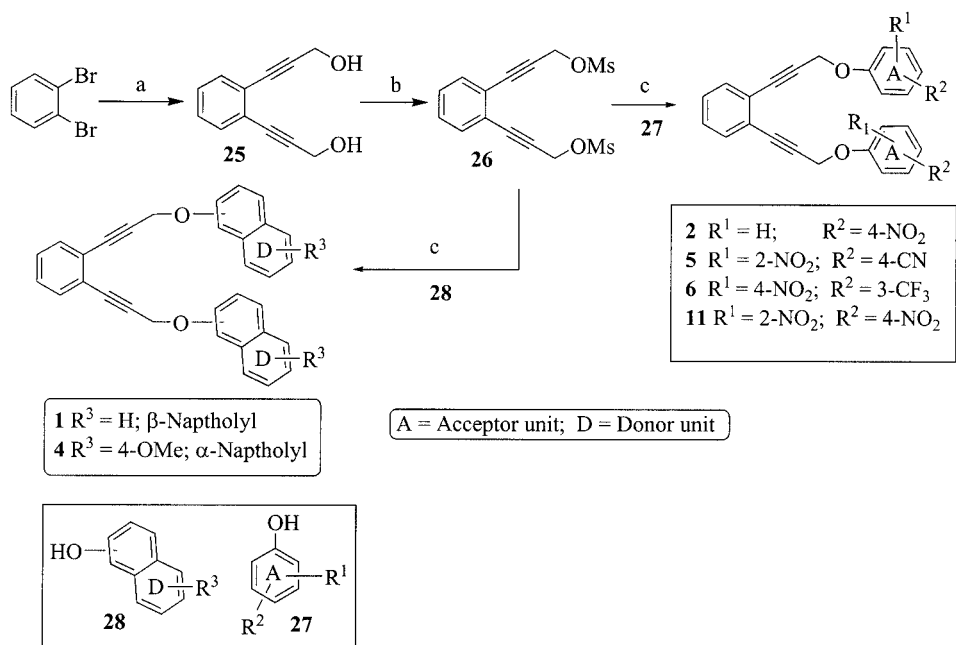
enediynes where the ene part comes from the aromatic double bond. Accordingly, we have followed the same reasoning here.

The synthesis of the target D/A compounds was first attempted by sequential Sonogashira coupling^[16] using appropriately substituted propargyl donors and acceptors. However, this strategy did not succeed as the highly basic

conditions employed in the coupling procedure led to deprotection of the acceptor molecule. The synthesis was finally achieved by sequential Sonogashira coupling of 1,2-dibromobenzene with propargyl and protected propargyl alcohols. The alcohol was then converted into the mesylate and reacted with the phenol (D or A). The THP protecting group was then taken off and mesylation followed by *O*-



Scheme 1. Synthesis of naphthoxy-based D/A enediynes. Reagents and conditions: a) Pd⁰, *n*BuNH₂, propargyl alcohol/THP-protected propargyl alcohol; b) MesCl/CH₂Cl₂; c) K₂CO₃/DMF; d) PPTS/EtOH.



Scheme 2. Synthesis of D/D and A/A enediynes. Reagents and conditions: a) Pd⁰, *n*BuNH₂, propargyl alcohol; b) MesCl/CH₂Cl₂; c) K₂CO₃/DMF/27 or 28.

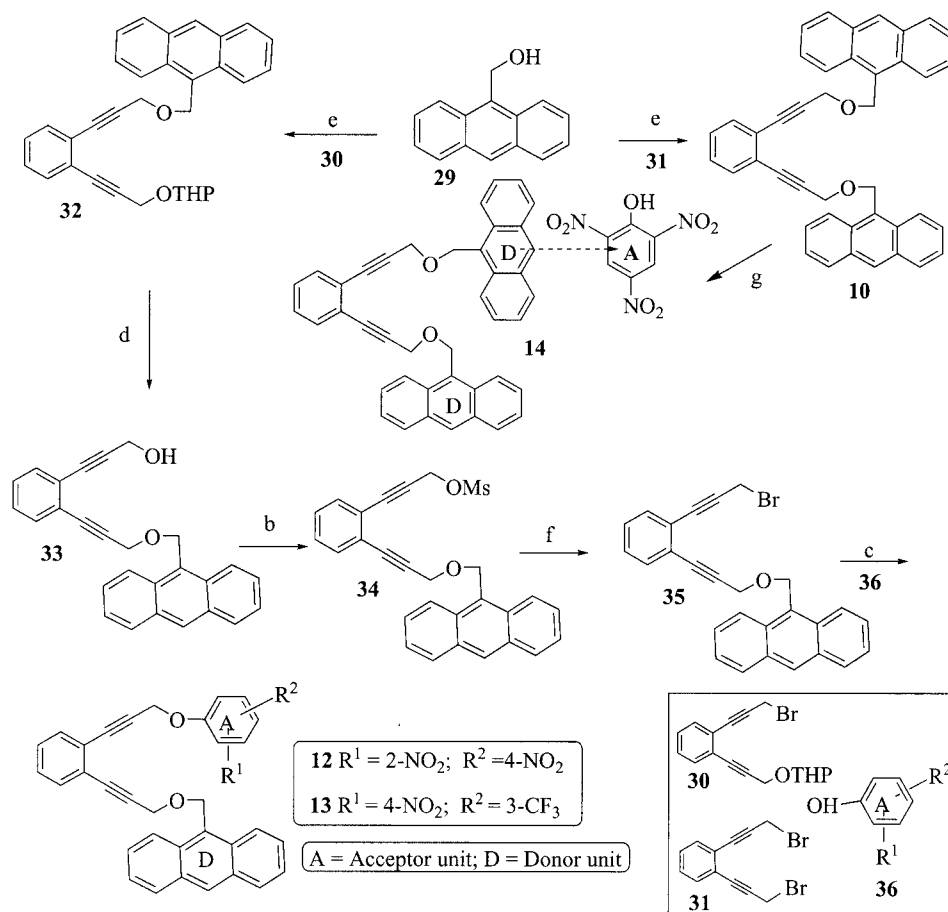
Table 1. DSC behavior of various enediynes.

Compd.	Aryl system	Onset temp. for BC/m.p. [°C]	Compd.	Aryl system	Onset temp. for BC/m.p. [°C]
1	2-naphthoxy (D) 2-naphthoxy (D)	168/116	8	4-methoxy-1-naphthoxy (D) 4-nitro-3-(trifluoromethyl)phenoxy (A)	121/oil
2	4-nitrophenoxy (A) 4-nitrophenoxy (A)	210/120	9	4-methoxy-1-naphthoxy (D) 4-nitrophenoxy (A)	152/151
3	2-naphthoxy (D) 4-nitrophenoxy (A)	161/101	10	anthracene-9-methoxy (D) anthracene-9-methoxy (D)	159/153
4	4-methoxy-1-naphthoxy (D) 4-methoxy-1-naphthoxy (D)	135/128	11	2,4-dinitrophenoxy (A) 2,4-dinitrophenoxy (A)	180/oil
5	4-cyano-2-nitrophenoxy (A) 4-cyano-2-nitrophenoxy (A)	245/243	12	anthracene-9-methoxy (D) 2,4-dinitrophenoxy (A)	125/123
6	4-nitro-3-(trifluoromethyl)phenoxy (A) 4-nitro-3-(trifluoromethyl)phenoxy (A)	205/116	13	anthracene-9-methoxy (D) 4-nitro-3-(trifluoromethyl)phenoxy (A)	119/oil
7	4-methoxy-1-naphthoxy (D) 4-cyano-2-nitrophenoxy (A)	126/oil	14	anthracene-9-methoxy (D) anthracene-9-methoxy-Picrate (A)	138/111

alkylation produced the target compounds with D/D, A/A, or D/A couples. Synthesis of the D/D and A/A pairs was carried out by double *O*-alkylation of the dimesylate **26** with two equivalents of phenol (donor or acceptor). In the case of anthracene-based enediynes, alkylation was carried out via the bromides as the yields were very poor using the mesylates. In one set of examples, we have used β -naphthol/4-methoxy- α -naphthol as the donor, and in another set the

anthracene unit of (9-anthracenyl)methanol as the donor. The acceptor molecules used were 4-nitro, 2,4-dinitro-, 4-cyano-2-nitro-, and 4-nitro-3-trifluoromethylphenols. The synthetic procedures are shown in Scheme 1, Scheme 2, and Scheme 3.

The onset temperatures for BC for these enediynes, namely the D/D, D/A, and A/A pairs, were determined by DSC^[17a] measurements, which were recorded for neat com-



Scheme 3. Synthesis of anthracene-donor-based enediynes. Reagents and conditions: b) MesCl/CH₂Cl₂; c) K₂CO₃/DMF/**36**; d) PPTS/EtOH; e) NaH/THF/**30** or **31**, reflux; f) LiBr/THF, room temp.; g) **10** in CH₂Cl₂/1 equiv. trinitrophenol.

pounds without any solvent. The results are shown in Table 1. For a series of D/D, D/A, and A/A compounds, the onset temperatures for BC for both the D/A and D/D combinations were found to be lower than for the A/A pair.^[17b] This reactivity difference can be explained on the basis of the proximity theory.^[18] In D/A compounds there is scope for formation of CT complexes, hence a flow of charge from the donor in one arm to the acceptor moieties in the other arm of the enediyne occurs through space. This forces the two acetylenic arms to come closer to each other, and, as a result, the cyclization temperature becomes lower. For the D/D enediynes this charge transfer is not possible,

but there is still a possibility of π -stacking interactions between the aromatic donor moieties in the two arms of the enediynes, which also can bring down the c,d distance and hence the cyclization temperature. On the other hand, the aromatic rings in the two arms of the A/A enediynes have negatively polarized charge densities and therefore remain far apart from each other due to coulombic repulsions. As a result, the c,d distance increases and hence the thermal cyclization barrier for the A/A enediynes in a given series is the highest. For example, the onset temperature for BC for CT complex **7** is 126 °C, about 9 °C less than for the D/D enediyne **4**, which cyclizes at 135 °C (Figure 2). On the other hand, the A/A enediyne **5** cyclizes at a much higher temperature (245 °C), thus emphasizing the role of CT complexation and π -stacking interactions.

The solution-phase kinetics were determined for one particular series, namely for **2** (A/A), **4** (D/D), and **9** (D/A), by heating a solution of the enediyne in a sealed tube at a preset temperature in CHCl₃ containing an excess of 1,4-cyclohexadiene and then taking the ¹H NMR spectrum at different times. In the NMR spectra, the signals for the two methylenes for the starting materials diminished over time while two new singlets corresponding to the methylenes of the newly formed naphthalene system, by BC, appeared and their signal intensity increased with time. For the D/D and D/A enediynes (**4** and **9**, respectively), the half-lives (determined at 90 °C) were found to be 11 and 18 h, respectively (Figure 3). The A/A enediyne **2** failed to cyclize at 90 °C even after heating for 102 h. In fact, it failed to cyclize even after heating for 5 h at 180 °C. The first-order rate constants for cyclization of **4** and **9** at 90 °C were calculated to be $5.15 \times 10^{-2} \text{ h}^{-1}$ and $3.02 \times 10^{-2} \text{ h}^{-1}$, respectively. These results again show the influences of CT and π -stacking interactions in the activation of BC. It is interesting to note that, in solution, the D/D enediyne **4** reacts about 1.6 times faster than the D/A enediyne **9**, which reveals that the π -stacking interaction in the solution phase is more pronounced than the charge-transfer interaction. In the solid

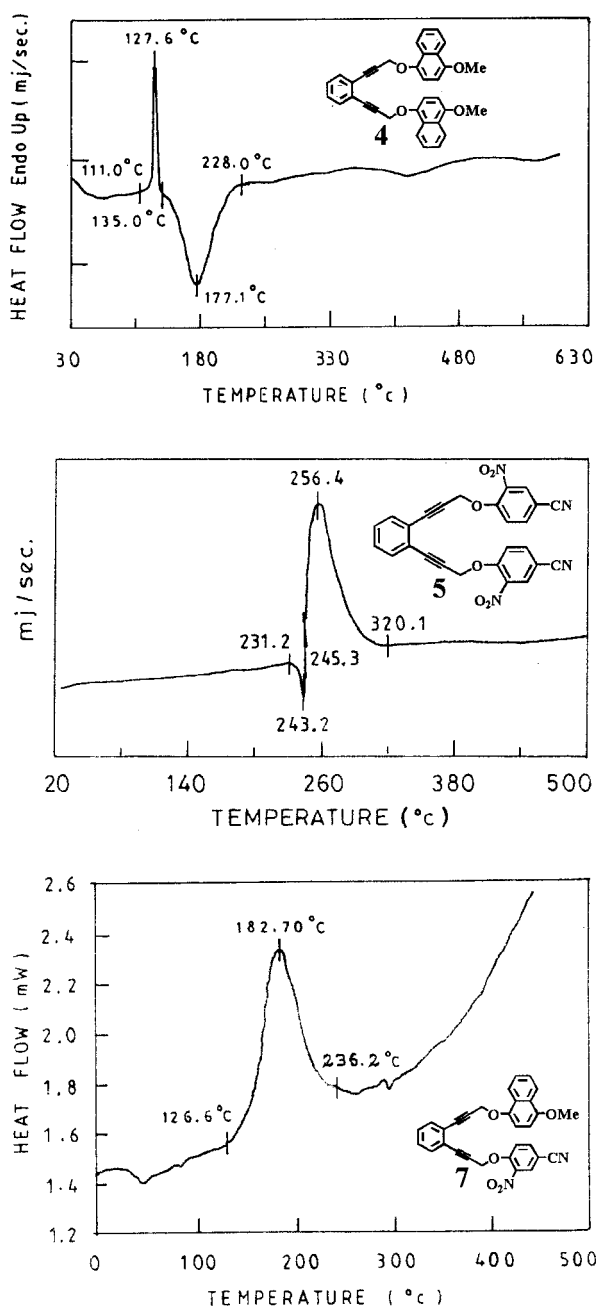


Figure 2. The DSC curves of the enediynes **4**, **5** and **7** with D/D, A/A and D/A pairs.

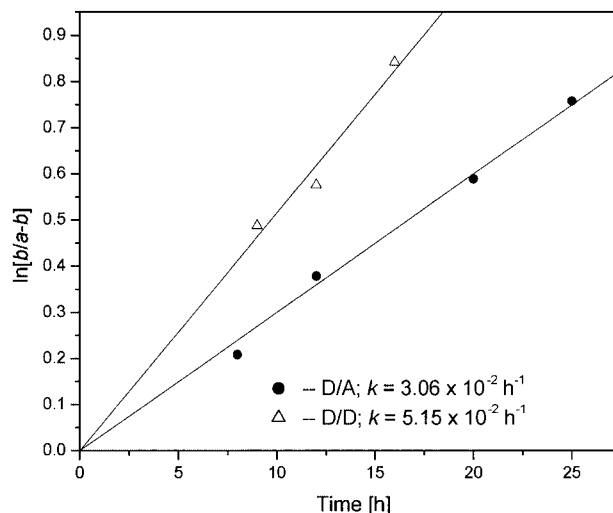
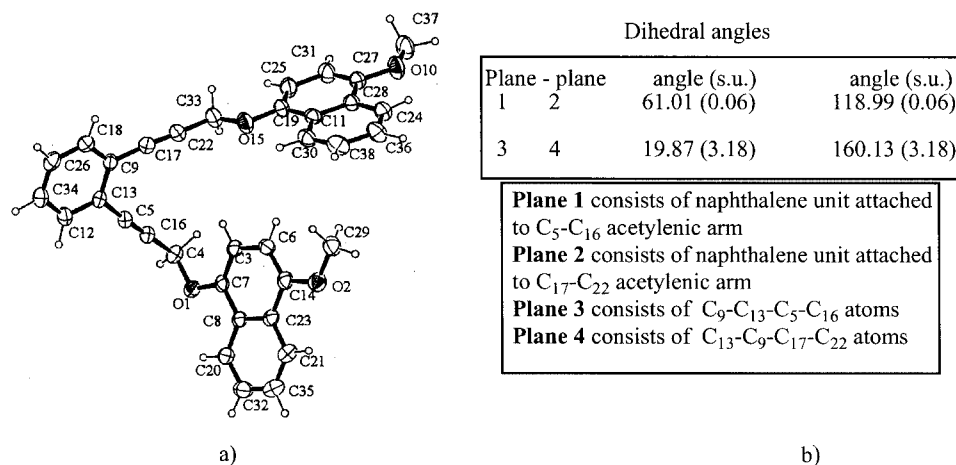


Figure 3. Solution-phase kinetics.

Figure 4. (a) ORTEP view and (b) dihedral angles for the D/D enediyne **4**.

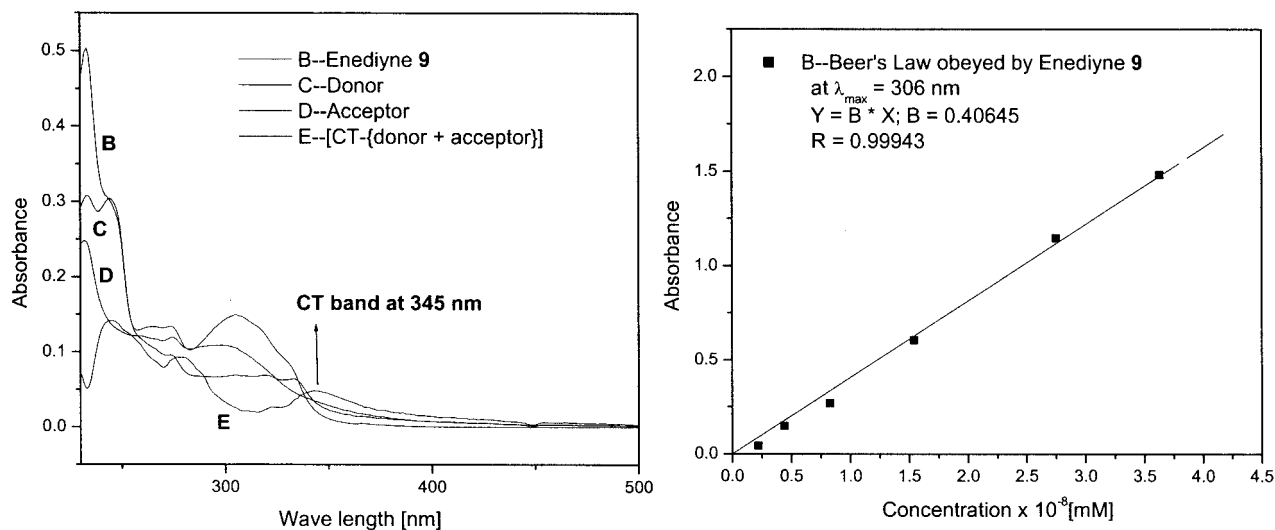
phase DSC, both these interactions have an almost similar influence on the onset temperature for BC.

The existence of π -stacking interactions in one of the D/D enediynes, namely **4**, was established by a single-crystal X-ray structure (Figure 4). The two naphthalene units face each other in a near orthogonal fashion, with the dihedral angle between them being 61.01°, thus indicating an intramolecular π -stacking interaction. The planes containing the acetylenic arms are out of planarity by 19.87°. The distances between the carbon atoms belonging to two different benzene rings range from 4.22 to 5.37 Å (Table 2), which supports the existence of π -stacking interactions between the aromatic moieties. The c,d distance came out to 3.85 Å, which is significantly lower than expected for an acyclic enediyne (ca. 4.12 Å).^[18] The packing structure shows that the molecule is mainly packed by hydrophobic interactions and is stabilized due to segregation of hydrophobic and hydrophilic interactions along the *c* axis; the aromatic rings are stacked along the *b* axis.

Table 2. Distances between the aromatic rings in enediyne **4**.

Carbon atoms	Distance [Å]	Carbon atoms	Distance [Å]
C3...C30	5.09	C6...C30	4.22
C3...C11	5.37	C6...C38	4.81
C3...C19	5.06	C14...C19	5.97
C6...C19	4.80	C14...C30	5.02
C6...C11	4.73	C14...C38	5.29

An intramolecular CT interaction is evident from the characteristic absorption and the associated color of the substance containing D/A units in two arms of the enediyne (**9**). A linear correlation is obtained between the absorbance of each D/A complex and the concentration, i.e., within the given concentration range the CT absorptions obey Beer's law. It is therefore evident that no intermolecular complexation is present (which would be expected to depend on the concentration squared), and, hence, all the absorbances are due to intramolecular complexation. In addition, the ap-

Figure 5. (a) UV spectra showing the appearance of the CT band, and (b) plot of absorbance vs. concentration of CT complex **9**.

pearance of a new, weak absorption band at 345 nm (due to partial transfer of π -electrons from the donor aromatic system to the acceptor) in the UV/Vis spectra of these materials, relative to the spectra of the separate donor and acceptor groups, provides further evidence for the formation of an intramolecular CT complex (Figure 5).^[19]

Thus, we have successfully demonstrated that charge-transfer or π -stacking interactions can enhance the cyclization kinetics. Repulsion between electron-deficient partners raises the activation energy. While the D/A enediynes become activated because of CT interactions, the enediynes with D/D arms also show greater reactivity than the corresponding A/A counterparts, possibly because of π -stacking interactions. It should be noted that in all the enediyne molecules the acceptor moieties are smaller than the donor aromatic systems. Thus, if only steric effects are operating we would expect the AA-enediynes to cyclize faster than their DD or DA counterparts. Since that is not happening, it is clear that the steric effects in these systems are overshadowed by CT and π -stacking interactions. Current efforts are aimed towards bringing down the activation barrier further by inducing stronger CT interactions.

Experimental Section

General: All NMR spectra were recorded in CDCl₃ unless otherwise stated.

Enediyne 1: Yield: 82%; reddish crystalline solid; m.p. 116 °C; λ_{\max} = 226 (s), 271 (w), 307 nm (w). ¹H NMR (200 MHz): δ = 4.75 (s, 4 H), 7.16 (d, J = 2.6 Hz, 2 H), 7.19–7.27 (m, 4 H), 7.33–7.45 (m, 6 H), 7.71–7.80 (m, 6 H) ppm. ¹³C NMR (50 MHz): δ = 56.42, 85.65, 87.94, 107.60, 118.85, 123.95, 125.01, 126.47, 126.97, 127.68, 128.33, 129.22, 129.43, 132.10, 134.38, 155.66 ppm. HRMS: calcd. for C₃₂H₂₂O₂ 438.1621; found 438.1624.

Enediyne 2: Yield: 82%; yellowish-white, crystalline solid; m.p. 120 °C; λ_{\max} = 233 (s), 273 (m), 305 nm (s). ¹H NMR (200 MHz): δ = 4.93 (s, 4 H), 7.10 (d, J = 9.0 Hz, 4 H), 7.30 (dd, J = 3.7, 5.4 Hz, 2 H), 7.42 (dd, J = 3.4, 8.7 Hz, 2 H), 8.23 (d, J = 9.0 Hz, 4 H) ppm. ¹³C NMR (50 MHz): δ = 56.95, 86.18, 86.48, 114.97, 124.32, 125.77, 128.81, 132.27, 142.01, 162.44 ppm. HRMS: calcd. for C₂₄H₁₆N₂O₆ 428.1009; found 428.1011.

Enediyne 3: Yield: 87%; reddish-white, crystalline solid; m.p. 101 °C; λ_{\max} = 267 (w), 274 (w), 306 nm (bs). ¹H NMR (300 MHz): δ = 4.54 (s, 2 H), 5.01 (s, 2 H), 6.89 (dd, J = 2.1, 7.1 Hz, 2 H), 7.27 (m, 4 H), 7.37 (dd, J = 4.4, 6.9 Hz, 2 H), 7.45 (dd, J = 3.7, 5.2 Hz, 2 H), 7.77 (t, J = 8.9 Hz, 3 H), 8.14 (dd, J = 2.1, 7.2 Hz, 2 H) ppm. ¹³C NMR (50 MHz): δ = 56.53, 56.73, 85.64, 86.23, 86.42, 88.00, 107.62, 114.90, 118.78, 124.06, 124.34, 125.06, 125.70, 126.58, 126.92, 127.66, 128.40, 128.70, 129.21, 129.52, 132.03, 132.12, 134.31, 141.87, 155.64, 162.44 ppm. HRMS: calcd. for C₂₈H₁₉N₄O₄ 433.1314; found 433.1317.

Enediyne 4: Yield: 89%; greenish, needle-shaped, crystalline solid; m.p. 128 °C; λ_{\max} = 235 and 245 (s), 269 (w), 274 (w), 315 nm (s). ¹H NMR (200 MHz): δ = 3.88 (s, 6 H), 4.91 (s, 4 H), 6.64 (d, J = 8.4 Hz, 2 H), 6.86 (d, J = 8.4 Hz, 2 H), 7.23–7.28 (m, 2 H), 7.41–7.52 (m, 6 H), 8.18–8.28 (m, 4 H) ppm. ¹³C NMR (50 MHz): δ = 55.63, 57.38, 85.52, 88.52, 103.03, 105.83, 121.79, 121.85, 125.15, 125.81, 125.97, 128.22, 132.00, 135.59, 135.95, 147.89, 153.63 ppm. HRMS: calcd. for C₃₄H₂₆O₄ 498.1832; found 498.1834.

Enediyne 5: Yield: 78%; yellow powder; m.p. 243 °C; λ_{\max} = 236 (s), 309 nm (w). ¹H NMR (200 MHz): δ = 5.16 (s, 4 H), 7.33 (dd, J = 3.5, 6.3 Hz, 2 H), 7.42 (dd, J = 2.7, 5.6 Hz, 2 H), 7.46 (d, J = 1.9 Hz, 2 H), 7.86 (dd, J = 2.0, 8.8 Hz, 2 H), 8.16 (d, J = 2.0 Hz, 2 H) ppm. ¹³C NMR (50 MHz): δ = 57.32, 84.15, 87.69, 105.91, 114.17, 116.10, 122.94, 129.15, 129.62, 132.34, 137.31, 147.22, 154.28 ppm. HRMS: calcd. for C₂₆H₁₄N₄O₆ 478.0914; found 478.0917.

Enediyne 6: Yield: 75%; yellowish solid; m.p. 116 °C; λ_{\max} = 232 (s), 271 nm (w). ¹H NMR (200 MHz): δ = 4.99 (s, 4 H), 7.27 (d, J = 2.6 Hz, 2 H), 7.33 (d, J = 4.1 Hz, 2 H), 7.42 (dd, J = 2.3, 8.6 Hz, 4 H), 8.04 (d, J = 9.0 Hz, 2 H) ppm. ¹³C NMR (50 MHz): δ = 57.33, 85.45, 86.99, 115.41 (CF₃), 117.27, 118.97, 124.01, 124.41, 127.93, 129.03, 132.44, 141.31, 160.53 ppm. HRMS: calcd. for C₂₆H₁₄F₆N₂O₆ 564.0756; found 564.0758.

Enediyne 7: Yield: 82%; reddish oil; λ_{\max} = 240 (s), 303 nm (s). ¹H NMR (200 MHz): δ = 3.98 (s, 3 H), 4.18 (s, 2 H), 5.12 (s, 2 H), 6.74 (d, J = 8.3 Hz, 1 H), 7.01 (d, J = 8.3 Hz, 1 H), 7.24–7.34 (m, 6 H), 7.43 (dd, J = 3.6, 5.7 Hz, 2 H), 7.51 (dd, J = 1.7, 3.2 Hz, 2 H), 8.27 (d, J = 9.2 Hz, 1 H) ppm. HRMS: calcd. for C₃₀H₂₀N₂O₅ 488.1373; found 488.1376.

Enediyne 8: Yield: 81%; reddish-yellow oil; λ_{\max} = 236 (s), 268 (w), 307 nm (b). ¹H NMR (200 MHz): δ = 3.95 (s, 3 H), 4.59 (s, 2 H), 5.07 (s, 2 H), 6.72 (d, J = 8.3 Hz, 1 H), 6.93 (dd, J = 2.7 Hz, 1 H), 6.98 (d, J = 3.2 Hz, 1 H), 7.26–7.31 (m, 3 H), 7.36–7.51 (m, 4 H), 7.86 (d, J = 9.0 Hz, 1 H), 8.23 (m, 2 H) ppm. ¹³C NMR (50 MHz): δ = 55.70, 57.20, 57.42, 85.42, 85.51, 87.09, 88.84, 103.03, 106.00, 115.63 (CF₃), 116.84, 121.77, 121.93, 124.12, 125.47, 125.97, 126.14, 126.40, 126.63, 127.83, 128.31, 128.87, 131.88, 132.14, 147.59, 150.26, 160.47 ppm. MS (EI): m/z = 531 [M⁺].

Enediyne 9: Yield: 78%; yellowish solid; m.p. 151 °C; λ_{\max} = 244 (s), 271 (w), 307 nm (s). ¹H NMR (200 MHz): δ = 3.95 (s, 3 H), 4.57 (s, 2 H), 5.04 (s, 2 H), 6.69 (d, J = 8.4 Hz, 1 H), 6.85 (dd, J = 2.2, 7.2 Hz, 2 H), 6.94 (d, J = 8.3 Hz, 1 H), 7.25–7.32 (m, 2 H), 7.36–7.53 (m, 4 H), 8.09 (dd, J = 2.0, 9.3 Hz, 2 H), 8.15–8.25 (m, 2 H) ppm. ¹³C NMR (50 MHz, CDCl₃ + CCl₄): δ = 55.95, 57.12, 57.64, 85.89, 89.98, 103.19, 106.02, 115.21, 122.20, 122.33, 126.02, 126.29, 126.47, 128.58, 128.99, 132.21, 132.38, 140.64, 147.82, 162.34 ppm. HRMS: calcd. for C₂₉H₂₁NO₅ 463.1420; found 463.1424.

Enediyne 10: Yield: 68%; yellow powder; m.p. 153 °C; λ_{\max} = 258 (s), 351, 368, and 387 nm (s). ¹H NMR (200 MHz): δ = 4.45 (s, 4 H), 5.53 (s, 4 H), 7.37–7.46 (m, 10 H), 7.62 (dd, J = 2.2, 5.6 Hz, 2 H), 7.95 (dd, J = 2.6, 5.5 Hz, 4 H), 8.37 (m, 6 H) ppm. ¹H NMR (200 MHz, [D₆]benzene): δ = 4.18 (s, 4 H), 5.45 (s, 4 H), 6.87 (dd, J = 3.3, 5.7 Hz, 4 H), 7.15–7.29 (m, 4 H), 7.46 (dd, J = 3.4, 5.6 Hz, 4 H), 7.72 (d, J = 8.1 Hz, 4 H), 8.08 (s, 2 H), 8.48 (d, J = 8.7 Hz, 4 H) ppm. ¹³C NMR (50 MHz): δ = 58.24, 63.48, 85.46, 89.72, 124.24, 124.86, 125.41, 126.18, 127.90, 128.28, 128.51, 128.85, 131.04, 131.27, 132.25 ppm. HRMS: calcd. for C₄₂H₃₀O₂ 566.2247; found 566.2245.

Enediyne 11: Yield: 78%; liquid; λ_{\max} = 233 (s), 257 (w), 294 nm (b). ¹H NMR (200 MHz): δ = 5.29 (s, 4 H), 7.31–7.53 (m, 6 H), 8.47 (dd, J = 2.6, 9.2 Hz, 2 H), 8.75 (d, J = 2.6 Hz, 2 H) ppm. MS (CI): m/z = 519 [MH⁺].

Enediyne 12: Yield: 78%; yellowish solid; m.p. 123 °C; λ_{\max} = 232 (s), 257 (s), 294 nm (b). ¹H NMR (200 MHz): δ = 4.66 (s, 2 H), 4.76 (s, 2 H), 5.64 (s, 2 H), 6.95 (d, J = 9.3 Hz, 1 H), 7.28–7.55 (m, 8 H, 4 × Ph-H), 7.79 (dd, J = 2.6, 5.2 Hz, 1 H), 7.93 (d, J = 8.0 Hz, 2 H), 8.32 (d, J = 2.9 Hz, 1 H), 8.37 (d, J = 9.8 Hz, 2 H), 8.44 (s, 1 H) ppm. HRMS: calcd. for C₃₃H₂₂N₂O₆ 542.1479; found 542.1481.

Enediynes 13: Yield: 78%; yellow oil; λ_{max} = 234 (s), 254 (w), 274 nm (w). $^1\text{H NMR}$ (200 MHz): δ = 4.61 (s, 2 H), 4.69 (s, 2 H), 5.70 (s, 2 H), 6.78 (dd, J = 2.9, 5.9 Hz, 1 H), 7.02 (d, J = 2.8 Hz, 1 H), 7.33–7.56 (m, 10 H), 7.95 (d, J = 1.7 Hz, 1 H), 8.43 (d, J = 7.8 Hz, 2 H), 8.49 (s, 1 H) ppm. $^{13}\text{C NMR}$ (50 MHz): δ = 57.35, 58.40, 67.74, 85.17, 85.52, 88.11, 89.89, 114.93 (CF_3), 116.52, 119.99, 123.20, 123.96, 124.55, 124.69, 124.99, 126.38, 128.33, 128.70, 129.00, 129.31, 131.04, 131.30, 132.08, 132.34, 133.34, 134.09, 145.03, 147.28, 160.39 ppm. MS (EI): m/z = 565 [M^+].

Enediynes 14: Red, leaf-shaped solid; m.p. 111 °C; λ_{max} = 233 (w), 257 (s), 386 nm (b). $^1\text{H NMR}$ (200 MHz, $[\text{D}_6]$ benzene): δ = 4.25 (s, 4 H), 5.48 (s, 4 H), 6.93 (dd, J = 3.4, 5.8 Hz, 4 H), 7.25–7.34 (m, 4 H), 7.51 (dd, J = 3.4, 5.6 Hz, 4 H), 7.76 (d, J = 7.9 Hz, 4 H), 8.03 (br. s, 2 H), 8.11 (br. s, 2 H), 8.50 (d, J = 8.5 Hz, 4 H) ppm.

- [1] R. S. Mulliken, *J. Am. Chem. Soc.* **1952**, *74*, 811–824.
 [2] H. F. Fisher, E. E. Conn, B. Vennesland, F. H. Westheimer, *J. Biol. Chem.* **1953**, *202*, 687–697.
 [3] B. Chance, *Mechanism of Enzyme Action*, Johns Hopkins Press, Baltimore, Md., **1954**, p. 433.
 [4] E. Racker, I. Krimsky, *J. Biol. Chem.* **1952**, *198*, 731–743.
 [5] G. Cilento, P. Gicsti, *J. Am. Chem. Soc.* **1959**, *81*, 3801–3802.
 [6] a) A. Foster, *Organic Charge-Transfer Complexes*; Academic Press: New York, **1969**; b) R. S. Mulliken, W. B. Person, *Molecular Complexes*; Wiley, New York, **1969**; c) M. L. Bundi, E. S. Jayadevappa, *Spectrochim. Acta* **1988**, *44*, 607–612.
 [7] a) D. J. Cram, R. A. Reeves, *J. Am. Chem. Soc.* **1958**, *80*, 3094–3103; b) D. J. Cram, R. H. Bauer, *J. Am. Chem. Soc.* **1959**, *81*, 5971–5977; c) D. J. Cram, D. L. Wilkinson, *J. Am. Chem. Soc.* **1960**, *82*, 5721–5723.
 [8] M. Raban, D. T. Durocher, *Tetrahedron Lett.* **1990**, *31*, 5125–5128.
 [9] W. Saenger, *Principles of Nucleic Acid Structure*, Springer-Verlag, New York.
 [10] S. K. Burley, G. A. Petsko, *Science* **1985**, *229*, 23–28.
 [11] a) A. Basak, S. Mandal, S. S. Bag, *Chem. Rev.* **2003**, *103*, 4077–4094; b) A. Basak, S. S. Bag, H. M. M. Bdoor, *Chem. Commun.* **2003**, *20*, 2614–2615; c) R. E. Gillard, F. M. Raymo, J. F. Stoddart, *Chem. Eur. J.* **1997**, *3*, 1933–1940; d) C. G. Claessens, J. F. Stoddart, *J. Phys. Org. Chem.* **1997**, *10*, 254–272; e) A. S. Shetty, J. Zhang, J. S. Moore, *J. Am. Chem. Soc.* **1996**, *118*, 1019–1027; f) G. B. McGuaghey, M. Gagné, A. K. Rappé, *J. Biol. Chem.* **1998**, *273*, 15 458–15 463.
 [12] G. B. Jones, P. M. Warner, *J. Am. Chem. Soc.* **2001**, *123*, 2134–2145.
 [13] I. V. Alabugin, *Abstracts of Papers, A.C.S. 2001*, 221st ORGN-448.
 [14] D. S. Rawat, J. M. Zaleski, *Chem. Commun.* **2000**, *24*, 2493–2494.
 [15] a) J. W. Grissom, T. L. Kalkins, H. A. McMillen, Y. Jiang, *J. Org. Chem.* **1994**, *59*, 5833–5835; b) K. C. Nicolaou, W.-M. Dai, Y. P. Hong, S.-C. Tsay, K. K. Baldrige, J. S. Siegel, *J. Am. Chem. Soc.* **1993**, *115*, 7944–7953.
 [16] a) K. Sonogashira, Y. Toda, N. Hagihara, *Tetrahedron Lett.* **1975**, *16*, 4467–4470; b) S. Takahashi, Y. Kuroyama, K. Sonogashira, N. Hagihara, *Synthesis* **1980**, 627–630.
 [17] a) B. König, H. Rutters, *Tetrahedron Lett.* **1994**, *35*, 3501–3504; b) The DSC curve for enediynes **9** shows two distinct exothermic peaks. This is not due to any impurity, as the $^1\text{H NMR}$ spectrum is clean. The experiment was therefore repeated twice. The genesis of these two peaks is not clear at this point; we have assigned the first exothermic peak as an indicator of onset of BC as the results obtained from solution-phase studies matched with the DSC results. Our studies with enediynes peptides^[11b] and pyridazine-based enediynes (A. Basak, S. S. Bag, P. A. Majumder, A. K. Das, V. Bertolasi, *J. Org. Chem.* **2004**, *69*, 6927–6930) revealed good correlation between DSC and solution-phase experiments. For enediynes that are solids, the onset of BC occurs after an endothermic peak, which indicates melting. For enediynes that are oils, there is only the exothermic peak. Thus we believe the cyclizations are all recorded under the same phase conditions.
 [18] K. C. Nicolaou, G. Zuccarello, Y. Ogawa, E. J. Schweiger, T. Kumazawa, *J. Am. Chem. Soc.* **1988**, *110*, 4866–4868.
 [19] D. Kost, N. Peor, G. Sod-Moriah, Y. Sharabi, D. T. Durocher, M. Raban, *J. Org. Chem.* **2002**, *67*, 6938–6943.

Received: September 21, 2004